Nanoscale Systems for Optical Quantum Technologies

Grant Agreement No: 712721
Start Date: 1st October 2016 - Duration: 36 months

D2.5 – Single readout ion

Deliverable:	D2.5
Work package:	WP2 Spin-atom-photon interfaces
Task:	2.2 Purcell enhancement of a single readout ion coupled to a qubit ion
Lead beneficiary:	ULUND
Type:	Report
Dissemination level:	Public
Due date:	30 June 2019
Actual submission date:	25 September 2019
Author(s):	Andreas Walther (ULUND)

This project has received funding from the European Union's Horizon 2020 research and innovation programme under grant agreement No 712721.

Version history

Version	Date	Author(s)	Description
V1	12/09/2019	A. Walther (ULUND)	First draft
V2	18/09/2019		Updated due to feedback
V3	24/09/2019		Updated due to feedback and submitted to EU

Table of Contents

Deliverable Description

This deliverable is a report on testing the idea of using a readout ion from one rare-earth (RE) species to readout the state of another species, acting as a qubit. A number of sub-questions can be formulated that is of interest for the RE quantum computing schemes:

- What is the expected benefit of involving two ion species, compared to one?
- What is the expected fluorescence count rate?
- Experimental verification of the properties of the chosen readout ion (Nd)
- Experimental measurement of the ion-ion coupling strength
- Implementation of the readout scheme at the single ion level

The focus of the investigation has been on using Nd as readout ion coupled to Pr ions as qubits, which was determined as the best pairing for a demonstration at this time. A large part of the experimental work has been to reach the single ion level, with the help of cavity Purcell enhancement effects, since this is the regime required for quantum computing. However, several of the questions listed above can and have been answered from measurements on ensembles or by theoretical simulations. In this report, we will list the progress on each of the parts.

Introduction and background to the results

In the first deliverable of NanOQTech (D2.1), it was suggested that for testing the readout-qubit ion coupling, the main scenarios should be Ce-Pr without cavity and Nd-Nd with cavity. Experimental work on Ce-Pr started already before the NanOQTech project and this report will cover the latest developments on this. It was stated in D2.1 that focusing on Nd as readout ion still required several experimental verifications. In particular, checking to see whether there were any spectral overlaps with transitions on other species, and whether the coherence time would be sufficiently good, considering that Nd is a Kramer's ion with electron spin, and thus more sensitive to external fields. The spectral overlap was measured and reported in NanOQTech deliverable D1.2, and it was found that Nd had significant overlap with Eu, but that the overlap with Pr lines were negligible. It has since then also been decided against the original potential idea of also using Nd as qubit ion, due in part to measurements under magnetic field and the difficulty of using the 7/2 nuclear spin isotopes as qubits. This experimental data will be discussed in the next section.

In order to answer the questions listed above in the deliverable description, and to determine the usefulness of the concept of coupling ions of different species, we have performed investigations along three different directions.

- Theoretical simulations and calculations have been used to answer some of the broader questions on potential and scalability, including expected benefits and expected signal strength.
- Experimental measurements on single ions is intended to be the main verification of the readout coupling scheme, since the final quantum computing protocols require the single ion regime. In order to achieve the goal, all optical components involved, including fibers and cavity used for the enhancement, must accommodate both the wavelength of the readout and of the qubit ion

simultaneously. We will describe the steps and decisions taken to ensure this, and report on the progress of the single ion interactions.

- Experimental measurements on ensembles were used to verify the characteristics of the Nd ions. In addition, detecting single RE ions at the 4f transitions in a manner that is consistent with the purpose of quantum computing has never been realized before, and carried a significant amount of experimental build-up. Thus, a parallel track of ensemble measurements were attempted to allow some information to be obtained earlier and at lower risk.

Results

Investigations on Ce-Pr interactions

Starting before NanOQTech, cross species interactions between Ce and Pr have already been achieved at ensemble level [1]. At the single ion level, it is still a remaining task to detect single Ce ions. Two issues have been identified, i) the Ce fluorescence is quenched by a mechanism believed to be trap state [2], and ii) a background fluorescence has been observed coming from the depth dimension of the crystals used. Within the duration of NanOQTech, attempts have been made to mitigate both effects. For i), the crystals were annealed by CNRS-CP at a temperature of 1200 °C over 24 h using an atmosphere of argon (95%) and hydrogen (5%). These conditions have been previously successful in removing trap states, although in another host crystal than ours [3]. However, in our host crystal, Y_2SiO_5, the annealing was unsuccessful in removing the trap states. For ii), it was tested whether smaller crystal sizes would eliminate the spurious background signal, but so far, no clear results have been obtained. Due to these issues, at this point, Ce-Pr is not our primary focus for readout-qubit ion coupling.

Theoretical simulations and calculations

In D2.1, it was suggested that same-species coupling might be simpler in terms of material growth and still good for quantum computing schemes. However, given the different strength of the different RE's, it was also pointed out that there may be substantial benefits from utilizing the different strengths in different ways, and thus separating the roles. In order to determine this benefit, calculations have been made on the potential fluorescence signal of a Purcell enhanced 4f transition of all major RE ions. Eu is intended to be the primary qubit ion, since the coherence properties (at least in other hosts) are very good, both on the optical transition where a T_2 of 2.6 ms [4] has been measured, and for the spin where 6 hours [5] have been reached at the ZEFOZ point (clock transition) and using dynamical decoupling. However, as can be seen from Fig. 1, there is a substantial difference in expected single ion fluorescence between Eu and that of the most fluorescing species, Nd, of about two orders of magnitude. The specific details of the calculation are given in the Appendix. The reason for this is that Nd has the largest transition dipole moment of the 4f transitions, and in addition has a high branching ratio to the ground state of about 20% [6], and finally a favorably long wavelength at 892 nm. At the same time, Nd is not expected to work that well as a qubit, since the coherence properties are worse and it only comes in two kinds of isotopes: either completely without nuclear spin, which is not favorable to long T_2, or with a spin of 7/2, which together with the necessary magnetic fields gives rise to a very complicated transition pattern. This suggests that there are very clear reasons for separating the roles in the

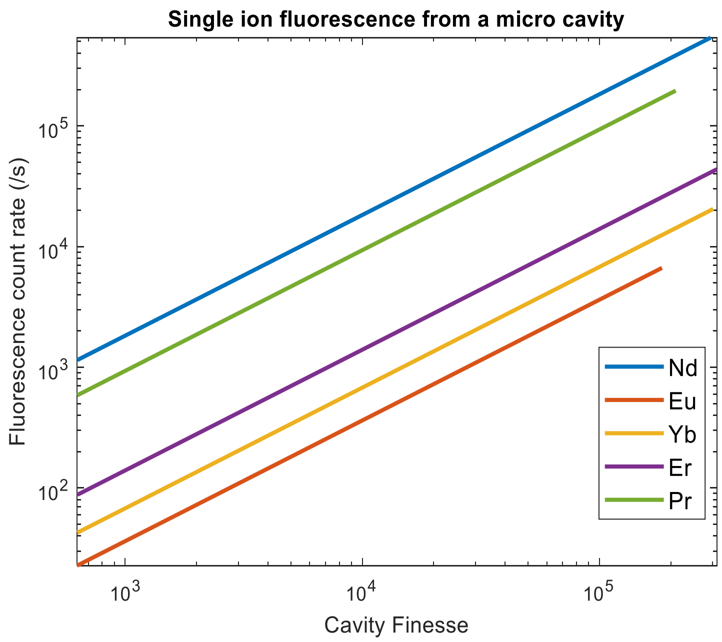

Figure 1. Expected single ion fluorescence signal using single photon counting from all major rare-earth ions. More details on the assumptions are given in the Appendix.

quantum computer, letting readout and qubit tasks be done by different species. In this particular host however, it was discovered that Nd and Eu does not co-dope well, since there are spectral overlaps between transitions (see D1.2), therefore Pr has been chosen as a test qubit ion instead.

Experimental measurements on ensembles

Since Nd is a Kramers' ion, i.e. an ion with an unpaired electron spin, it is significantly more sensitive to the surrounding fields compared to Eu. Even if the coherence properties are more important for the qubit, even a dedicated readout ion would need a sufficiently long coherence time. This is because a long coherence time corresponds to a narrow linewidth, and the narrower the linewidth is, the smaller can the interaction shift from the dipole-blockade effect be, in order for the qubit ion to impart control on the readout. Therefore, it was important to verify that the coherence properties of Nd in the Y_2O_3 host

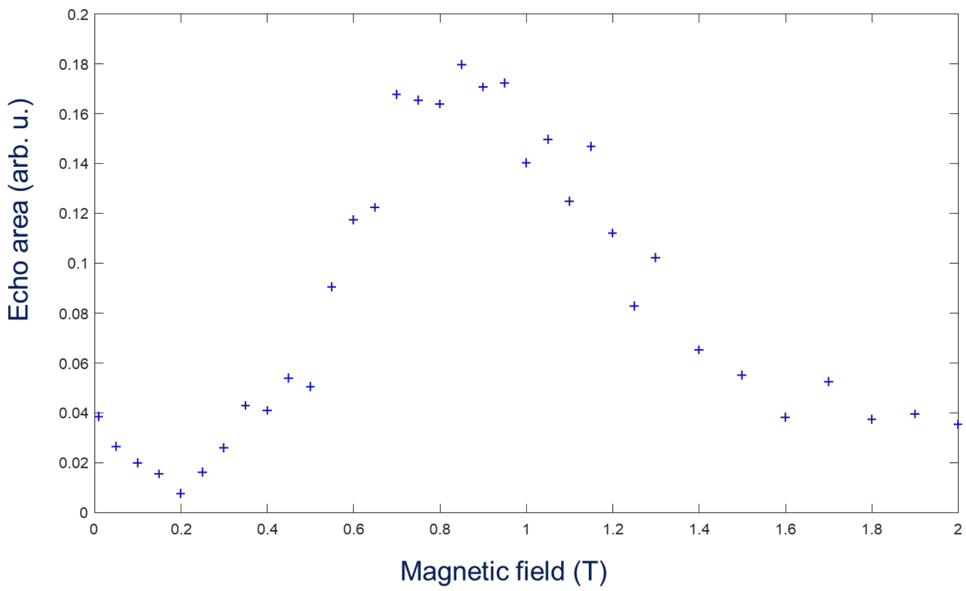

Figure 2. Photon echo signal strength as a function of applied magnetic field.

was sufficiently good. In order to perform this measurement as early as possible (before the single ion regime had been reached), these measurements were performed on ensembles of ions. The sample was a non-transparent ceramic of pressed together micron-sized crystallites containing 100 ppm doping concentration of Nd, measured by a 4f-imaging setup onto an APD. Note that the measurements performed thus give an ensemble average. The fluorescence signal revealed an excited state lifetime of about 350 µs, and an inhomogeneous line of about 5 GHz was obtained. In order to measure the coherence time, a photon echo sequence was applied at varying levels of magnetic field in order to probe the sensitivity of the electron spin, as can be seen in Fig. 2.
It was found that the coherence increases strongly with magnetic field up to a maximum at about 0.9 T. At this point the coherence time was T_2 = 5.7 µs, which is very similar to the coherence values for other RE species in the same host [7]. The reason for the similarity, despite large differences in oscillator strength, is probably that the coherence is primarily limited by material properties such as defects. It will be important for the future success of these materials to improve the T_2, but for the current initial demonstrations, this value is good enough.

Another experimental run, with nanocrystals in powder form, was also performed. This time, Nd was co-doped with Pr in order to allow the inter-species coupling strength to be measured. The fluorescence lifetime of Nd was again measured and found to be about 540 µs, i.e. significantly longer than for the ceramics. This can be explained by the fact that the refractive index for a powder with plenty of empty space surrounding the emitting ions is lower, causing the emission mode to be weaker (this effect is investigated for this material in Ref. [8]). It turned out however, that the nano-crystals were significantly more difficult to obtain an optical coherent signal from, such that the available laser power was too low to measure the coupling strength between the ions by photon echo techniques. This is because the effective amount of crystal material is much lower for a loose powder compared to a compressed ceramic. Rather than spend more time on ensemble measurements, that were meant to give a quick answer, the focus was shifted to the more long-term viable single instance setup.

Experimental setup to detect single RE ions

The core of the experimental setup to detect single RE ions is a micro-sized Fabry-Perot cavity that enables Purcell enhancement of the fluorescence signal. The fundamental technology to build such a micro-cavity assembly was transferred from partner KIT, and has been explained in a previous deliverable (D1.1). Changes to that design had to be made to accommodate a smaller sample space and to allow both wavelengths of the two different species to interact with ions inside the cavity. The design and construction of the various parts are discussed below. In addition to this, nano-crystals that are co-doped with both Nd (100-200 ppm) and Pr (1000 ppm) have been obtained from the partner CNRS-CP. The radius of the nano crystals are about 70-110 nm, which should give only low scattering losses from the cavity, given our finesse and wavelength.

Dual wavelength design for coatings and fibers

Since Nd would be the readout ion, the Purcell enhancement must be maximized for this wavelength (892 nm). For the qubit ions on the other hand, no enhancement is actually required, provided that a single pass of the beams give sufficient Rabi frequency to enable fast gates. In addition, having a cavity effect on both wavelengths would give no guarantee that both resonances could be hit at the same time, which would constitute a significant risk. Therefore the high-reflective coatings forming the mirrors in the cavity, was designed to be fully transmissive on the qubit wavelength (619 nm). A number of fibers were produced in collaboration with partner KIT, with different radii of curvature (giving different cavity mode characteristics) and of various lengths. The fibers were subsequently coated for high reflectivity by a company, Laser Optik. Two different reflectivities were chosen, R=99.5 and R=99.9%, corresponding to cavity finesses of about 600 and 3000 respectively. New fibers with even higher finesse could be produced at a later stage, when an active cavity length stabilization system can be added to the assembly, but according to Fig. 1, the available finesses should already yield a sufficient fluorescence count rate. At the same time, the coatings were designed to yield a maximum of the electric field amplitude about 100 nm from the surface, such that the doped nano crystals embedded in a thin layer of PMMA should be placed at that field maximum.

Another wavelength dependent element of the setup was the cut-off wavelength of the fiber that acts as one of the mirrors. 619 nm is far enough away from 892 nm, that any fiber that has a low enough cut-off to allow 619 nm to propagate in single mode, would have a large amount of bending losses at 892 nm. Since the signal would come at 892 nm, this was deemed too high a price, and consequently a cut-off wavelength of 800 nm was chosen. This means that the qubit wavelength is propagating through the fiber in the few mode regime, but since there is no cavity effect on the qubit wavelength, this should not be an issue. Different modes in fiber can also experience dispersion, propagating at different speeds, however, this effect is negligible with the short fiber lengths in our setup.

Design and construction of the micro-cavity assembly

The primary challenge for the design of the mounting assembly was to have it highly stable, i.e. a situation where the two opposing mirrors of the cavity do not move relative to each other, and at the same time have control of as many degrees of freedom as possible in terms of moving parts. In the end, we found a solution where the two lateral axes are

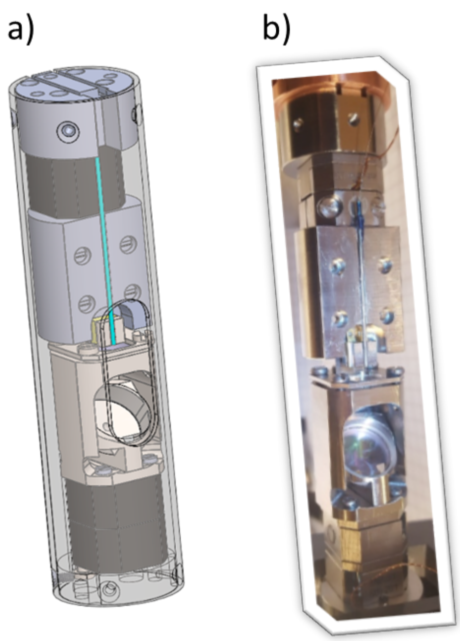

Fig. 3. a) design of the narrow micro-cavity assembly (<25 mm diameter) and b) the completed construction fully in titanium.

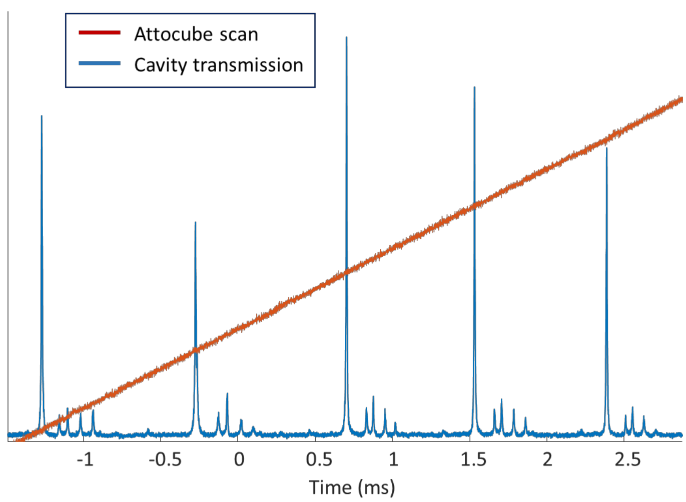

Fig. 4. Cavity fringes as measured from the transmitted signal.

scannable via x/y attocube positioners for searching the sample surface, and where the depth is scannable both by a z attocube and separately by a piezo. The SolidWorks design can be seen in Fig. 3 a) and the final machined construction in part b). A part from the piezo and the optics, all parts of the assembly are made in titanium (same material as the attocubes), in order to minimize the thermal contractions and the strain caused by cooling the setup down to 2 Kelvin. Due to the limitation of the assembly diameter of <25 mm, control of some degrees of freedom had to be forsaken, including angle tuning of the fiber tip with respect to the flat mirror, instead relying on sufficient mounting precision.

The assembly with the fiber cavity has been tested by coupling light into the fiber and observing both the reflection and the transmission signal, while scanning the length of the cavity. A trace of the fringes of the cavity is seen in Fig. 4. Here, we observe repeating sets of peaks, where the main peaks correspond to the desired cavity spatial mode and the smaller peaks correspond to spurious spatial modes. These come from an imperfectly placed angle of the fiber tip, which is difficult to fix in our setup due to the limited size available for these adjustments. However, from the relative power in the modes, we see that the coupling to the desired mode is much stronger and sufficiently good. We can also use the data to measure the finesse of the setup, since $F = \delta_{fwhm}/\Delta_{fsr}$ where δ_{fwhm} is the width of the lines and the free spectral range, Δ_{fsr}, is their separation. In different setups, using the coatings design for F = 600, we measure finesses of 200-600, meaning we are able to fully realize the potential of the coatings. Furthermore, the stability of the setup is such that the transmission at the center of a cavity mode, stays within one linewidth at a time scale of seconds to minutes. Even the initially modest value of the cavity finesse of 600, should give enough signal to detect single Nd ions.

Conclusions and outlook

We have designed and completed the construction of all parts of the setup required to detect single Nd ions and to investigate the interactions between readout ions and qubit ions. As a summary, we again list the questions given in the description of this document at the start, this time with a summary of the answers that were obtained:

- What is the expected benefit of the involving two ion species, compared to one?
    - Given the large difference in expected fluorescence count, there is a significant gain in using two species over only one. An additional gain is the fact that single-shot readout techniques, such as the one described in Ref. [9] becomes available.
- What is the expected fluorescence count rate?
    - About 1000-10000 photons/s with present technology, and about 10^5 photons/s with the next generation of cavities within a few years.
- Experimental verification of the properties of the chosen readout ion (Nd)
    - Coherence time and lifetime is sufficiently good to act as a readout ion.
- Experimental measurement of the ion-ion coupling strength
- Implementation of the readout scheme at the single ion level

Of the listed questions, only the tasks related to the last two were not fully reached, since we were unable to perform the final experiments with the finished setup in time for this deliverable, mainly due to issues with our supply of liquid helium and a broken attocube positioner. The outlook for being able to perform the planned experiments within the coming months is very good, as both issues are about to be resolved as of September 2019. With all information available at the present though, the readout scheme looks very promising for rare-earth quantum computing.

Appendix

In order to calculate the expected fluorescence signals for the different RE species, a number of experimental assumptions had to be made. This section gives details on those assumptions.

Most of the equations for calculating the cavity parameters, such as cavity-fiber coupling efficiency, cavity mode diameter, scattering losses due to particle size etc., was taken from [10]. The expression for the final enhanced decay rate into the cavity mode was taken from [11]. It was assumed that the nano-crystals had a particle radius of about 40 nm and were surrounded with PMMA to reduce the index of refraction contrast. This gave only small losses due to Rayleigh scattering for most of the wavelengths and finesse values. Different single photon counting APD detectors (quantum efficiency and dark counts) were chosen according to the optimum for each wavelength, although superconducting detectors were not used. The frequency width of the laser has been assumed to be at most $\frac{1}{\pi T_2}$, such that there is no extra power broadening. A doping concentration of about 100-1000 ppm was used, which would mean that only a single ion is available in any nano-crystal at this frequency interval. Losses due to output coupling from cavity to fiber was included as well as losses due to detector efficiency, although no other optical losses were taken into account. RE ion parameters, such as lifetime and branching ratio, were picked from literature or from measurements performed by the partners within NanOQTech.

References

[1] Y. Yan, J. Karlsson, L. Rippe, A. Walther, D. Serrano, D. Lindgren, M. Pistol, S. Kröll, P. Goldner, L. Zheng, J. Xu, *Phys. Rev. B* **2013**, *87*, 184205.
[2] J. Karlsson, A.N. Nilsson, D. Serrano, A. Walther, P. Goldner, A. Ferrier, L. Rippe, S. Kröll, *Phys. Rev. B* **2016**, *93*, 224304.
[3] T. Kornher, K. Xia, R. Kolesov, N. Kukharchyk, R. Reuter, P. Siyushev, R. Stöhr, M. Schreck, H.-W. Becker, B. Villa, A.D. Wieck, J. Wrachtrup, *Applied Physics Letters* **2016**, *108*, 053108.
[4] F. Könz, Y. Sun, C.W. Thiel, R.L. Cone, R.W. Equall, R.L. Hutcheson, R.M. Macfarlane, *Phys. Rev. B* **2003**, *68*, 085109.
[5] M. Zhong, M.P. Hedges, R.L. Ahlefeldt, J.G. Bartholomew, S.E. Beavan, S.M. Wittig, J.J. Longdell, M.J. Sellars, *Nature* **2015**, *517*, 177.
[6] B.M. Walsh, J.M. McMahon, W.C. Edwards, N.P. Barnes, R.W. Equall, R.L. Hutcheson, *J. Opt. Soc. Am. B* **2002**, *19*, 2893.
[7] A. Perrot, P. Goldner, D. Giaume, M. Lovric, C. Andriamiadamanana, R.R. Goncalves, A. Ferrier, *Phys. Rev. Lett.* **2013**, *111*, 203601.
[8] B. Casabone, J. Benedikter, T. Hümmer, F. Oehl, K. de Oliveira Lima, T.W. Hänsch, A. Ferrier, P. Goldner, H. de Riedmatten, D. Hunger, *New J. Phys.* **2018**, *20*, 095006.

[9] A. Walther, L. Rippe, Y. Yan, J. Karlsson, D. Serrano, A.N. Nilsson, S. Bengtsson, S. Kröll, *Phys. Rev. A* **2015**, *92*, 022319.
[10] D. Hunger, T. Steinmetz, Y. Colombe, C. Deutsch, T.W. Hänsch, J. Reichel, *New Journal of Physics* **2010**, *12*, 065038.
[11] A. Reiserer, G. Rempe, *Rev. Mod. Phys.* **2015**, *87*, 1379.